Dalton Transactions

ROYAL SOCIETY OF CHEMISTRY

PAPER

View Article Online
View Journal | View Issue

Cite this: *Dalton Trans.*, 2026, **55**, 2452

Electrophilic lithium carbazolide as an efficient trap for organolithium species: complexes containing monomeric *n*-BuLi, *t*-BuLi and Me_3SiCH_2Li units

Mikhail A. Bogachev,[a] Alexander N. Selikhov,*[a,b] Anton V. Cherkasov,[a] Rinat R. Aysin[b] and Alexander A. Trifonov*[a,b]

Received 23rd November 2025,
Accepted 29th December 2025

DOI: 10.1039/d5dt02800k

rsc.li/dalton

The lithiation reactions of superbulky 3,6-di-*tert*-butyl-1,8-bis-(2,4,6-triisopropylphenyl)-9*H*-carbazole (**1**) with a two-fold molar excess of *n*-BuLi, *t*-BuLi, or Me_3SiCH_2Li in heptane afford the binuclear lithium complexes [Carb$^{2,4,6\text{-}iPr}$Li(μ^2-*n*-Bu)Li] (**2**), [Carb$^{2,4,6\text{-}iPr}$Li(μ^2-Me_3SiCH_2)Li] (**3**), and [Carb$^{2,4,6\text{-}iPr}$Li(μ^2-*t*-Bu)Li] (**4**) in 80, 90, and 56% yields. The single-crystal X-ray diffraction studies revealed that **2–4** are binuclear ionic complexes comprising the alkyl group μ^2-bridging two lithium centers, one of which is also η^6-coordinated with the phenyl fragment of the carbazolyl ligand. For complexes **2** and **3**, the binuclear structures are retained in solution as evidenced by ^{1}H, ^{13}C, ^{7}Li, and ^{1}H DOSY NMR spectroscopy. QTAIM and NCI data reveal a difference in the strength of Li–C interactions between **2–4**, which are weaker for **4**, and rationalised the *t*Bu-substituted **4** prone to dissociation.

Introduction

Organolithium reagents have been essential components in organic and organometallic chemistry since the pioneering work by Wilhelm Schlenk and Joanna Holtz in 1917.[1] Moderate cost and relative ease of synthesis, combined with high Brønsted basicity and solubility in common organic solvents have made organolithium reagents the gold standard among other polar hydrocarbyl metal derivatives for over 100 years.[2] It is difficult to overestimate the importance of commercial *n*-BuLi and *t*-BuLi, produced in thousands of tons per year, and used as nucleophiles,[3] deprotonating (or lithiation) and reducing agents in organic synthesis,[4] and universal tools for introducing lithium into organic substrates (*via* metal–halogen exchange).[5]

However, in solution, organolithium reagents form aggregates of varying nuclearities *via* bridging Li–C bonds.[6] Hence, the reactivity of RLi complexes in synthesis varies enormously, depending not only on the structure of the hydrocarbyl radical (R), but also on the aggregation degree.[7] It is known that in non-basic solvents, organolithium compounds tend to assemble oligomeric structures, which stabilize the polar and reactive Li–C bonds.[6d,e,7]

The simplest lithium-hydrocarbyl complex forms tetrameric $(MeLi)_4$ units, linked to each other through very strong intercluster contacts, thus causing the insolubility of methyllithium in non-coordinating solvents, like pentane or hexane.[8] Besides MeLi, higher *tert*-butyllithium and ethyllithium form tetrameric structures $(t\text{-BuLi})_4$ and $(EtLi)_4$,[9] whereas *n*-butyllithium,[9a] i-propyllithium,[10a] cyclohexyllithium[10b] and Me_3SiCH_2Li form hexamers $[RLi]_6$ in the crystalline state, adopting an octahedral geometry.[10]

Moreover, recent studies have shown the existence of an octameric structure of *n*-BuLi in various hydrocarbon solvents.[11]

Numerous interactions of R^- moieties with multiple lithium centers, accompanied by smearing of the negative charge, ultimately lead to a decrease in the reactivity of $[RLi]_n$ aggregates compared to hypothetical RLi "naked" monomers.[6a,d] Also, it has been established experimentally and computationally that a decrease in the degree of aggregation leads to an increase in the ionicity of the Li–C bond and hence, the monomeric RLi should be the most reactive.[6a,c,d,7]

Therefore, the design of well-defined alkyllithium monomers is of crucial importance not only for providing deeper insight into the mechanism of RLi-mediated reactions, but also for unlocking novel reactivity patterns.[12]

Two opposing strategies are used to split organolithium aggregates into monomer units: complexation of lithium with N,O- and N,N-basic ligands (the most common approach) and, conversely, chelation of the carbanion fragment with electro-

[a]*G. A. Razuvaev Institute of Organometallic Chemistry, Russian Academy of Sciences, 603950 Nizhny Novgorod, Russian Federation. E-mail: trif@iomc.ras.ru*
[b]*A.N. Nesmeyanov Institute of Organoelement Compounds, Russian Academy of Sciences, 119334 Moscow, Russian Federation*

philic metal centers (Fig. 1). According to the first approach, neutral Lewis-basic donors block lithium coordination sites, thereby kinetically stabilizing monomeric complexes. Recently, the monomeric methyllithium has been obtained due to the application of bulky N,N-chelating macrocyclic ligands: [Li(CH_3)(κ^3-*N*,*N*′,*N*″-DETAN)] (DETAN = (*N*,*N*′,*N*″-tris-(2-*N*-diethylaminoethyl)-1,4,7-triaza-cyclononane)) and [Li(CH_3)(Me_3TACN)] (Me_3TACN = 1,3,7-trimethyl-1,3,7-triazacyclononane.[13] To date, only three reports describe the synthesis and structure of monomeric $LiCH_2SiMe_3$, stabilized by bidentate and tridentate amine ligands: [Li(CH_2SiMe_3)(PMDTA)],[14] [Li(CH_2SiMe_3)(R,R-TMCDA)][6b] and [Li(CH_2SiMe_3)(κ^3-*N*,*N*′,*N*″-Me_6Tren)].[14] The tetrameric structure of the bulkiest (*t*-BuLi)$_4$ readily dissociates in the presence of various bases, affording monomeric units: *t*-BuLi(THF)$_3$, *t*-BuLi((−)-sparteine), *t*-BuLi(R,R-TMCDA), *t*-BuLi(TEEDA), and *t*-BuLi(T*t*BuTAC) (*t*-BuTAC – 1,3,5-tri-*tert*-butyl-1,3,5-triazacyclohexane).[15]

In contrast to lithium complexation with bases, another disaggregation strategy involves multimetallic chelation of the carbanion moiety (Fig. 1b).[16] Thus, in complexes [(THF)$_3$Li$_3$(μ-Me){(*t*-BuN)$_3$S}] and [Mo$_2${(μ-H)Li(THF)(μ-CH_3)}$_2$(AdDipp$_2$)$_2$] (AdDipp$_2$ = HC(NDipp)$_2$; Dipp = 2,6-diisopropylphenyl), the methyl carbanion, although monomeric, acts as a bridging ligand shared by multiple metal sites (Mo and Li).[16a,b]

However, despite being perhaps the most well-known, widely used and most explored organometallic reagent, to date, no isolated monomeric complexes of *n*-BuLi have been reported. The splitting of the six-nuclear aggregate (*n*-BuLi)$_6$ through complexation with Lewis bases affords tetramers and dimers, accompanied by undesirable metalation of the base itself.[15e,16c,17]

In this work, we present the unexpected formation of bimetallic lithium carbazolyl complexes, containing monomeric alkyllithium units (*n*-Bu, Me_3SiCH_2 and *t*-Bu).

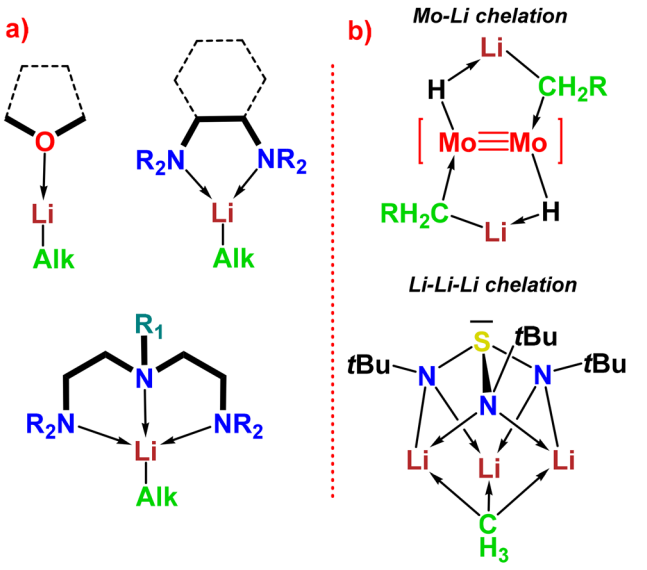

Fig. 1 Approaches for the dissociation of (RLi)$_n$ aggregates: (a) the use of neutral N,O-bases and (b) multimetallic chelation of the carbanionic fragment with electrophilic metal centers.

Results and discussion

Synthesis, structure and reactivity

Interest in the development of low-coordinate alkali metal complexes is dictated by their enormous potential in synthesis and catalysis due to the presence of vacant metal coordination sites and exceptional reactivity. Among the ligands enabling stabilization of the challenging one-coordinate alkali metal complexes, the carbazolyl platform is an excellent candidate due to the facile modification of its steric demand.[18] Furthermore, the introduction of bulky aryl substituents into the 1,8-positions of carbazole provides extremely high steric shielding of the metal center, which is necessary for the stabilization of coordinatively unsaturated complexes.[19] Inspired by these findings, and considering the importance of designing a sterically shielded pocket defined by the flanking *ortho*-substituents, we have been targeting the "superbulky" monoanionic 1,8-disubstituted carbazol-9-yl ligand (**1**) bearing 2,4,6-triisopropylaryl groups (Scheme 1).[20]

Initial attempts to synthesize the target superbulky carbazole *via* cross-coupling of 3,6-di-*tert*-butyl-1,8-dibromocarbazole with aryl boronic acid failed due to its insufficient nucleophilicity. The Kumada cross-coupling is complicated by the formation of a large amount of the THF ring cleavage by-product (see the SI for details).[20] It is likely that the highly electrophilic two-coordinate magnesium carbazolide, formed during the process, activates the THF molecule, preparing it for subsequent insertion into the Mg–$N_{carbazole}$ bond. However, the Negishi cross-coupling reaction with excess arylzinc reagent affords carbazole **1** in an excellent yield of 80% (Scheme 1).

The ^{1}H NMR monitoring (C_6D_6, 23 °C) revealed that the deprotonation reaction of **1** with *n*-BuLi (1 : 1 molar ratio) is non-selective and leads to the targeted lithium carbazolide (80%) along with the homobimetallic complex [Carb$^{2,4,6\text{-iPr}}$Li(μ^2-*n*-BuLi)Li] (**2**, 10%) consisting of lithium carbazolide μ-bridged by an *n*-butyl fragment with the second lithium ion. The starting carbazole **1** (10%) is also detected in the mixture.

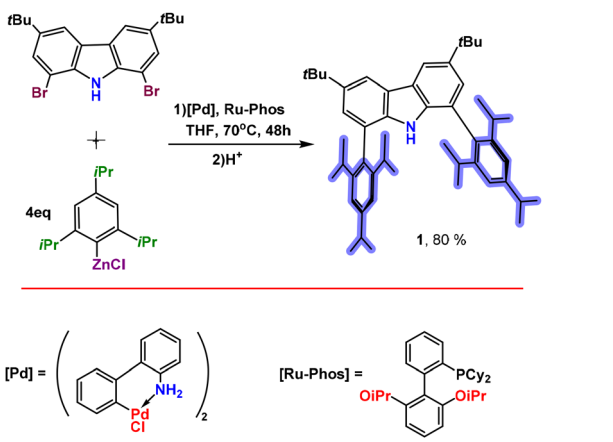

Scheme 1 Synthesis of 3,6-di-*tert*-butyl-1,8-bis-(2,4,6-triisopropylphenyl)-9*H*-carbazole (**1**).

In C_6D_6 solution, lithium carbazolide probably exists as an adduct [Carb$^{2,4,6\text{-iPr}}$Li](C_6D_6), the ^{1}H NMR spectrum of which corresponds to the recently published complex with prothiobenzene.[20] This complex [Carb$^{2,4,6\text{-iPr}}$Li](C_6H_6) was also isolated as the only product of thermolysis of complex **2** in benzene (see below).

Analogous reaction of **1** with Me_3SiCH_2Li also gives a mixture of compounds [Carb$^{2,4,6\text{-iPr}}$Li]/[Carb$^{2,4,6\text{-iPr}}$H]/[Carb$^{2,4,6\text{-iPr}}$Li(μ^2-Me_3SiCH_2Li)Li] (**3**) in a ratio of 72 : 14 : 14% (see SI, Fig. S7). Heating of the NMR sample at 70 °C for 1 h results in complete consumption of carbazole with quantitative formation of lithium carbazolide [Carb$^{2,4,6\text{-iPr}}$Li](C_6D_6). Repeating reaction **1** with a two-fold molar excess of *n*-BuLi or Me_3SiCH_2Li on a preparative scale in heptane medium at 23 °C results in the exclusive formation of homobimetallic complexes **2** and **3** in 80% and 90% yields after recrystallization from *n*-heptane (Scheme 2). Analogous reaction of *t*-BuLi with **1** in heptane also affords binuclear complex **4** in 58% yield.

However, deprotonation of **1** with the simplest alkyllithium reagent, MeLi, in cyclohexane does not afford the desired complex [Carb$^{2,4,6\text{-iPr}}$Li(μ^2-MeLi)Li]. As we have previously shown, instead of methyllithium, electrophilic lithium carbazolide traps cyclohexane and forms an unusual κ^2-alkane complex (Carb$^{2,4,6\text{-iPr}}$)Li(κ^2-C_6H_{12}). This is probably due to the fairly strong intercluster agostic interactions in the MeLi tetramer, which prevent its dissociation.[8]

Complexes **2–4** crystallize from a heptane solution in the form of large, colorless crystals that are extremely air- and moisture-sensitive. Six lipophilic i-Pr groups together with *t*-Bu groups of the carbazole backbone make these complexes highly soluble in non-coordinating aliphatic or aromatic solvents (benzene, toluene, heptane, and hexane).

According to single crystal X-ray diffraction (SC XRD) data, complexes **2–4** crystallize with two crystallographically independent complex molecules in the asymmetric part of the unit cell. The molecular structures of the complexes are shown in Fig. 2a–c, and the crystal data and refinement details are summarized in Table S1. Complexes **2–4** are binuclear homometallic base-free lithium carbazolides, containing two lithium centers differing in their coordination environment. One of the lithium ions Li(1) in **2–4** is located in the carbazolyl plane and bonded to the amide nitrogen atom with short, almost identical Li–N bonds (1.936(11), 1.959(11) Å (**2**), 1.913(5), 1.945(5) Å (**3**), and 1.937(5), 1.948(5) Å (**4**)). In **2–4**, these distances are expectedly longer than those in the previously described one-coordinate carbazolides and amides: *t*-Bu_2CarbAr$_2$Li (Toluene) 1.877 Å (Ar = 3,5-*t*-BuC_6H_3),[19g] *t*-Bu_2Carb(2,4,6-i-$Pr_3C_6H_2$)$_2$Li(1-octene) 1.841(15)–1.896(3) Å,[20] and [(i-Pr)$_3$Si]$_2$NLi 1.872(3) Å.[21] Moreover, in **2–4**, this Li ion is linked with the α-carbon of the RLi carbanion, which is μ^2-bridging two electrophilic lithium centers. The alkyl moieties are located in a cavity formed by two bulky 2,4,6-i-$Pr_3C_6H_2$ substituents, preventing aggregation into high-order associates. The distances between "amide" lithium and the alkyl carbons are 2.11(2), 2.163(12) Å in **2**, 2.140(6), 2.167(6) Å in **3**, and 2.170(6), 2.175(5) Å in **4**, respectively. These distances are much longer than the distances from R^- to the second lithium atom due to the different coordination environment of lithium atoms.

The distances from the alkyl carbon to the second Li ion are: 2.00(3), 2.018(12) Å in **2**, 2.025(6), 2.058(6) Å in **3**, and 2.063(6), 2.074(6) Å in **4** and are much shorter than the typical values of covalent Li–C bonds in other alkyl lithium derivatives: [(*n*-BuLi)$_2$·PMDTA]$_2$ (Li–C: 2.121(6)–2.225(6) Å),[17] [Li(CH$_2$SiMe$_3$)(PMDTA)] (2.113(2) Å),[14] and [(*t*-BuLi)$_2$·3THF] (Li–C: 2.2241(17)–2.3250(17) Å).[15a] Moreover, these Li–α-C distances

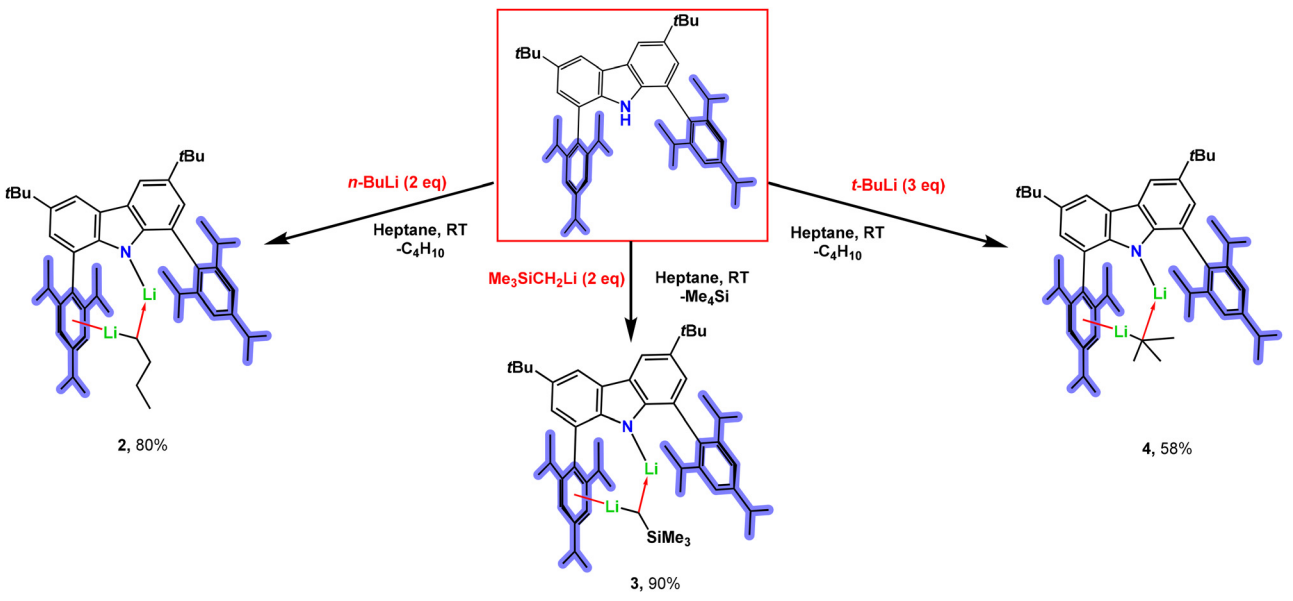

Scheme 2 Synthesis of complexes **2–4**, containing the monomeric alkyllithium fragment.

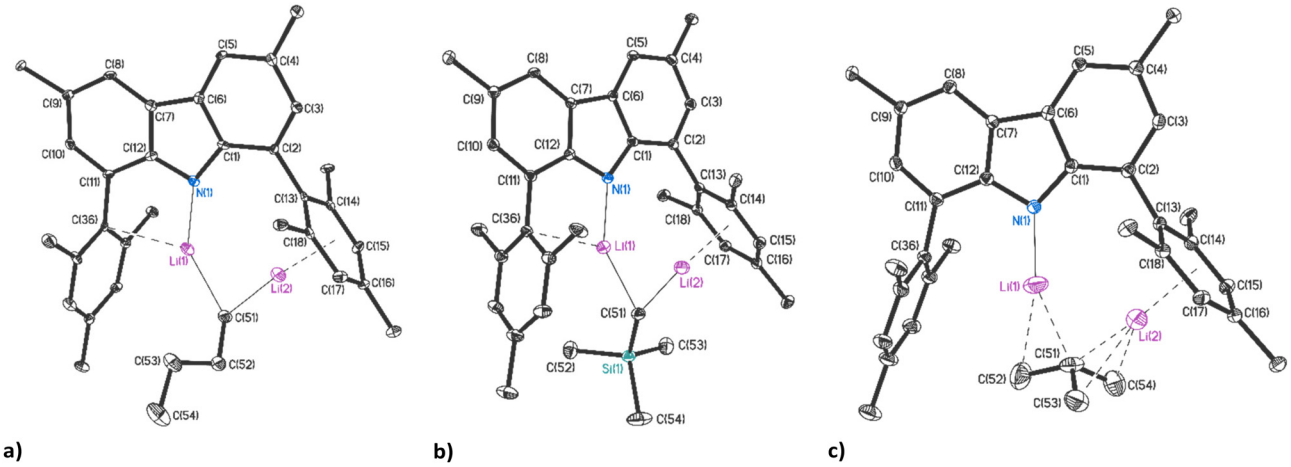

Fig. 2 Molecular structures of complexes **2** (a), **3** (b), and **4** (c). Thermal ellipsoids are given at the 30% probability level. Methyl groups of *t*-Bu- and i-Pr substituents, and hydrogen atoms are omitted for clarity.

are the shortest among all published lithium alkyl complexes of any nuclearity and any lithium coordination number (Table 1).[6]

Only two monomeric *tert*-butyl lithium complexes with very bulky N,N-chelate *t*-BuLi·(R,R)-TMCDA (2.064(15) Å)[15c] and cyclic 1,3,5-tri-*tert*-butyl-1,3,5-triazacyclohexane ligands [(*t*-BuTAC)(*t*-BuLi)] (2.083(2) Å)[15e] have similar bond lengths. According to a charge density investigation,[22] these findings are mainly attributed to strong electrostatic attraction between two highly charged atoms (negatively charged carbanion and positively charged Li cation).

Interestingly, both Li–C distances become longer with increasing bulk of the alkyl group *n*-Bu < Me_3SiCH_2 < *t*-Bu, most likely due to the extrusion of the alkyl ligand from the cavity of the carbazolyl ligand. Moving from complex **2** to complex **4**, the lipophilic cage limited by six isopropyl substituents monotonously expands, reaching a maximum for complex **4** (see below).

The coordination unsaturation of the second lithium ion Li(2) is compensated by a series of non-covalent interactions with one flanking the tris(isopropyl)phenyl moiety. The Li–C(Ar) distances in **2–4** are close and vary from 2.33(2) to 2.51(2) Å for **2**, from 2.322(6) to 2.481(6) Å for **3**, and from 2.338(6) to 2.430(6) Å for **4**. Thus, lithium–arene interaction features a η^6-mode. In addition, the electron deficient nature of the Li(N) center in **2** and **3** also manifests in its interaction with one *ipso*-carbon atom of the flanking aryl moiety, Li(1)–C_{ipso}: 2.53(2), 2.62(2) Å in **2**, and 2.525(6), 2.657(6) Å in **3**.

However, in complex **4**, the bulkiness of the $(CH_3)_3C^-$ group prevents this interaction, resulting in a much longer Li–C_{ipso} distance (2.898(5), 2.944(6) Å) and the realization of an additional interaction of Li(1) with the methyl group of the carbanion (Li(1)–C(52) 2.431(7) Å). Two other methyl groups are involved in the coordination of Li(2) with resulting distances of 2.381(7) and 2.496(6) Å. Interestingly, in the second crystallographically independent molecule of **4**, the coordination of Me_3C^- is realized in a different way: each of the Li^+ cations is bound to only one methyl group (Li(1)–C(52) 2.345(6) Å, Li(2)–C(53) 2.317(6) Å). The third group is located far from the cations (Li(1)–C(54) 3.056(6) Å and Li(2)–C(54) 2.797(7) Å) and does not participate in the interaction.

In our opinion, the combination of the electrophilic low-coordinate lithium center with the finely tailored ligand, which provides shielding of this center turned out to be a suitable tool for the stabilization of the monomeric alkyllithium units. Furthermore, due to the presence of *ortho*-i-Pr substituents, free rotation of the aryl rings around the C–C bonds is hampered. They are closely orthogonal to the carbazolyl het-

Table 1 Selected distances (Å) and chemical shifts in NMR spectra (ppm) for **2–4** [a]

	Complex					
Parameter	**2**	**3**	**4**	$(n\text{-BuLi})_6$	$(Me_3SiCH_2Li)_6$	$(t\text{-BuLi})_4$
Li(1)–α-C[b]	2.11(2)	2.140(6)	2.170(6)			
Li(2)–α-C[b]	2.00(3)	2.025(6)	2.063(6)	2.137(3)[9a]	2.17(4)[10c]	2.147(17)[9a]
$\delta(^1H)$–α-CH_2	−1.71	−2.97		−0.57[9a]	−2.16[29]	
$\delta(^{13}C)$–α-C	7.48	−9.17	13.30	11.8[30]		10.5[30]
$\delta(^7Li)$	−1.04	−1.34	−1.47			

[a] For comparison, published parent base-free complexes are given. [b] The shortest distances are given.

erocycle (76.0(2)–87.2(2)° in **2**, 75.23(6)–88.26(7)° in **3**, and 80.18(6)–87.95(5)° in **4**) and form a lipophilic pocket enabling the assembly of base-free hetero-aggregates containing a monomeric alkyl lithium block. The formation of similar products has been previously described in kinetically induced partial metalation of arenes containing a DMG (directing metalating group) with *n*-butyllithium. The resulting kinetic hetero-aggregates $\{Li_4[C_6H_3\text{-}(CH(Et)NMe_2)_2\text{-}2,6]_2(n\text{-}Bu)_2\}$,[23] $\{Li_4[CH_2C_6H(CH_2NMe_2)_2\text{-}2,6\text{-}Me_2\text{-}3,5]_2(n\text{-}Bu)_2\}$,[24] $\{Li_4[CH(SiMe_3)C_6H(CH_2NMe_2)_2\text{-}2,6\text{-}Me_2\text{-}3,5]_2(n\text{-}Bu)_2\}$,[25] $\{Li_4[CH_2Si(Ph)_2CH_2N(CH_2CH_2\text{-}OMe)_2]_2(n\text{-}Bu)_2\}$,[26] and $\{Li_4[C_6H_4CH(Me)NMe_2\text{-}2]_2(n\text{-}Bu)_2\}$[27] have a tetranuclear structure and contain two *n*-butyllithium units.

A structure with bimetallic μ^2-Li_2 chelation of the *n*-Bu fragment is reported for the mixed alkyl–aryl lithium complex $\{Li(n\text{-}Bu)\}_2(LiMes^*)_2$ (Mes* = 2,4,6-*t*-$Bu_3C_6H_2$) obtained through lithium halide exchange.[16c]

In addition, hetero-aggregates containing sterically more demanding alkyl lithium species are also described.[28] To the best of our knowledge, complex **2** is the first structurally characterized complex containing a monomeric *n*-butyl lithium moiety. Moreover, complexes **3** and **4** represent a rare example of alkyllithium hetero-aggregates containing an alkyl group bulkier than *n*-Bu.

The NMR spectra of complexes **2** and **3** in C_6D_6 solution suggest that the solid-state structures persist in solution. Despite the nonsymmetric binding of the alkyllithium moiety to the lithium carbazolide, the ^1H and $^{13}C\{^1H\}$ NMR spectra exhibit single sets of signals for these fragments. In the ^1H NMR spectra, the chemical shifts of the carbazolyl protons for both complexes **2** and **3** are almost identical, indicating a weak electronic influence of the nature of the coordinated RCH_2Li moiety (R = C_3H_7, $SiMe_3$). Restricted rotation of the aryl substituents around the C–C bond is evidenced by the presence of two sets of signals attributed to the *ortho*-i-Pr groups in the ^1H NMR spectra of **2** and **3**.

The methyl protons of the *ortho*-i-Pr substituents give rise to the doublets with chemical shifts of 1.10 and 0.96 ppm for **2**, and 1.10 and 0.98 ppm for **3**, respectively. In C_6D_6 solution, complexes **2** and **3** proved to be rather stable: no dissociation or substitution of RCH_2Li by the solvent was detected. The ^1H DOSY spectra of **2** and **3** in C_6D_6 (SI Fig. S11 and Fig. 3b) clearly demonstrate that the lithium carbazolide and the corresponding RCH_2Li form a stable complex since the protons from both units display the same diffusion coefficient ($D = 9.42 \times 10^{-9}$ m^2 s^{-1} for **2**, 9.26×10^{-9} m^2 s^{-1} for **3**).

The high field shift of the signals corresponding to the α-methylene protons relative to the parent complexes $(n\text{-}BuLi)_6$ and $(Me_3SiCH_2Li)_6$ (Fig. 3a) is a characteristic feature of complexes **2** and **3**. The methylene groups associated with the Li ions appear as a sharp triplet at −1.71 ppm (**2**) and a singlet at −2.97 ppm (**3**). The corresponding shifts for $(n\text{-}BuLi)_6$ and $(Me_3SiCH_2Li)_6$ are 1.14 and 0.81 ppm, respectively (Table 1).[9a,29] Complexes **2** and **3** are characterized by the most upfield shifted signal corresponding to the carbanion α-CH_2 protons among all known complexes. The signals of the α-CH_2 carbons in $^{13}C\{^1H\}$ spectra are strongly broadened and upfield shifted in comparison with other alkyllithium species;[2,6] no characteristic C–Li coupling was observed. The ^7Li NMR spectra display a single resonance at −1.04 (for **2**) and −1.34 ppm (for **3**), despite the fact that two different environments were observed for Li^+ ions in the X-ray crystal structure. Most likely a rapid exchange between two different lithium sites is the reason for the broadening of the α-CH_2 signals in the ^{13}C NMR spectra.

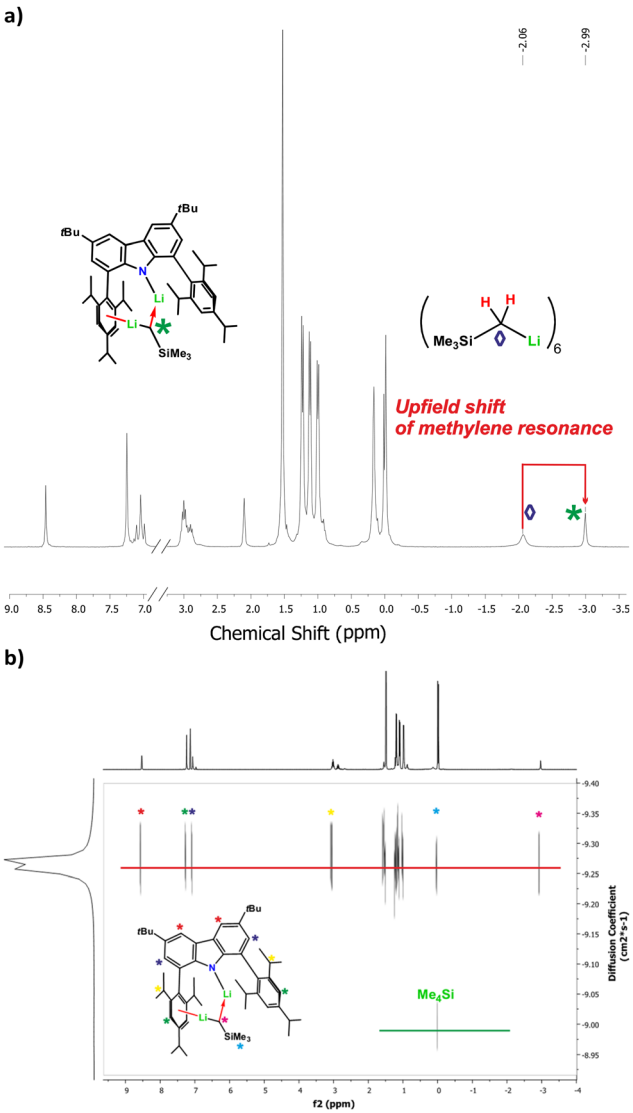

Fig. 3 (a) ^1H NMR spectrum of **3**, presenting the upfield shift of the α-CH_2 signals relative to $[Me_3SiCH_2Li]_6$ in toluene-d_8 at room temperature. (b) ^1H DOSY spectrum of **3** in C_6D_6.

In order to detect the retention of the unsymmetric metal–ligand bonding in solution, variable temperature NMR studies were carried out for complex **3** in the range of 213–343 K (toluene-d_8). A temperature decrease to 213 K leads to a slight drift of the *o*-C*H*Me_2 and *p*-C*H*Me_2 signals (from 3.02 and 2.91 ppm at 298 K to 3.05 and 2.85 ppm at 213 K); however, the averaged "symmetrical" bonding mode of the carbazolyl

ligand remains unchanged (see the SI, Fig. S18–S20). No signal splitting was observed even at 203 K. In contrast, when the sample was heated to 343 K, a slight broadening of the signals corresponding to 3,5-CH-aryl, Me_3Si, and CH_2 protons occurred; however, no splitting of the signals was observed. The ^{7}Li NMR spectrum shows a single resonance that indicates the equivalence of lithium ions on a NMR timescale. These observations most likely result from a dynamic process involving fast scrambling of the carbazolyl ligand and the Me_3SiCH_2 radical over the Li_2-faces.

Unexpectedly the ^{1}H NMR spectrum of complex **4**, recorded in benzene-d_6 at room temperature, is indicative of the presence of two different compounds in a 1 : 1 ratio. The addition of excess *t*-BuLi does not lead to an equilibrium shift. In the ^{1}H NMR spectrum, the signal belonging to the *t*-BuLi protons of **4** appears as a sharp singlet at 0.49 ppm (SI, Fig. S25). In the $^{13}C\{^1H\}$ NMR spectrum, the tertiary carbon $(CH_3)_3C$ gives rise to a strongly broadened singlet at 13.30 ppm (C_6D_{12}, 293 K). The second set of signals in the ^{1}H NMR spectrum corresponds to the product of substitution of the *t*-BuLi fragment by the C_6D_6 molecule [Carb$^{2,4,6\text{-iPr}}$Li](C_6D_6) (SI, Fig. S25). Surprisingly, the ^{1}H DOSY NMR spectrum of **4** recorded in cyclohexane-d_{12} also provides evidence of the complex dissociation (SI, Fig. S26) and formation of [Carb$^{2,4,6\text{-iPr}}$Li](κ^2-C_6D_{12}).[20]

Taking into account the exceptionally weak coordination properties of aliphatic hydrocarbons, this observation seems to be rather unusual. Recently, we have reported a facile olefin substitution by both benzene and cyclohexane in lithium carbazolide complexes.[20] Most likely the excessive bulkiness of *t*-BuLi leads to a weakening of its bonding with lithium carbazolide and facilitates substitution with benzene or cyclohexane. This suggestion is confirmed by the DFT calculations of dissociation energies for the obtained complexes, which are presented below. Recrystallization of **4** from benzene affords complex [Carb$^{2,4,6\text{-iPr}}$Li(η^2-C_6H_6)] (**5**)[20] in 22% yield (see the Experimental section). Unfortunately, all the attempts to obtain single crystals of the analogous complex with cyclohexane by crystallization of **4** from C_6H_{12} failed. The structure of complex **5** is completely consistent with the previously published report.[20]

Complexes **2–4** containing a formally monomeric hydrocarbyllithium fragment turned out to be surprisingly highly thermally stable.

They are inert towards activation of C–H bonds of toluene and benzene at room temperature and even when heated at 80 °C for 2 h. The probable reason for the low reactivity of complexes **2–4** in metalation reactions is low nucleophilicity of the carbanion caused by its coordination with two lithium acceptor centers and the two-electron three-center nature of the resulting Li–C bond. On the other hand, the carbanions in these complexes are reliably shielded by 2,4,6,-i-$Pr_3C_6H_2$ substituents from an attack by proton-containing substrates.

Heating complexes **2** and **3** in benzene or toluene at 100 °C for 24 h leads to the decomposition of the alkyl lithium component and the formation of the related η^2-arene complexes **5** and **6** in 56 and 75% yields, respectively (Scheme 3). Thermolysis of complex **2** in benzene proceeds *via* β-hydride abstraction with the formation of 1-butene and LiH as expected products, which were identified by GC/MS and acid–base titration, respectively. Thermolysis of complex **3** in toluene affords Me_4Si and unidentifiable lithium-containing products. No formation of BnLi was detected by ^{1}H NMR spectroscopy.

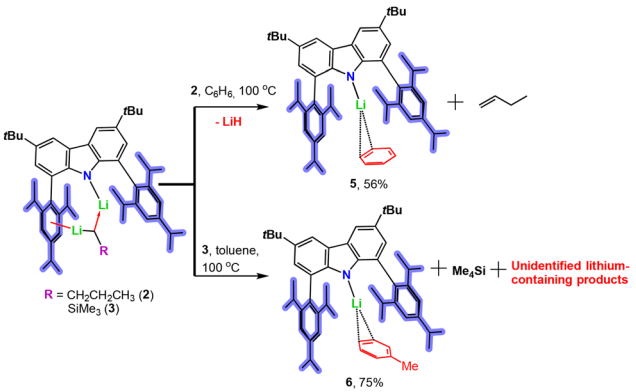

Scheme 3 Thermolysis of complexes **2** and **3** in C_6H_6 and toluene solutions.

Complex **6** crystallizes in the monoclinic $P2_1/c$ space group and its structure is depicted in Fig. 4. As in **2–4**, the lithium cation in **6** is coordinated to the carbazolyl ligand *via* the amide nitrogen atom (Li–N 1.910(10) Å) and one Li–C_{ipso} short

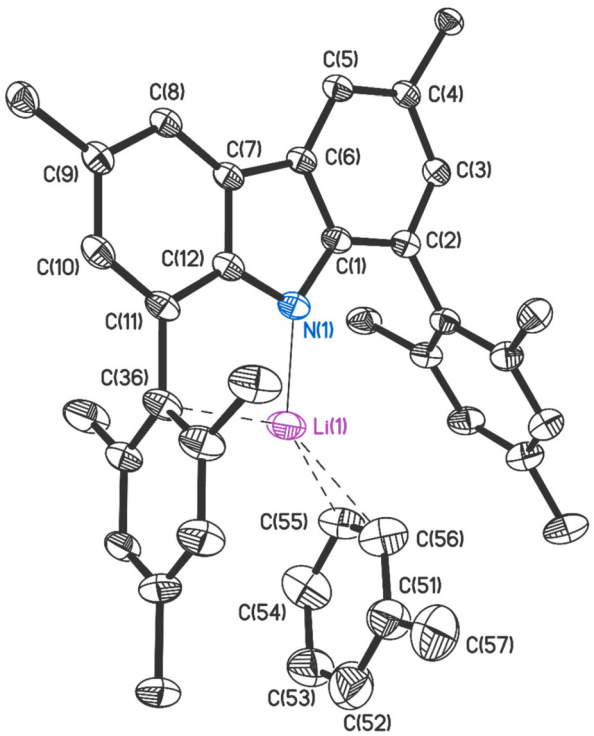

Fig. 4 Molecular structure of complex **6**. Thermal ellipsoids are given at the 30% probability level. Methyl groups of *t*-Bu- and i-Pr substituents, and hydrogen atoms are omitted for clarity.

contact (2.43(2) Å). The most notable structural feature of **6** is the marginally asymmetric η^2-coordination of the toluene molecule to the lithium center. The lithium cation and the toluene molecule are disordered by two sites. Unlike numerous reported examples of lithium arene π-complexes,[16c,31] the lithium cation in **6** exhibits only two short Li–$C_{toluene}$ contacts 2.27(2) and 2.34(2) Å, while other Li–$C_{toluene}$ distances are in the range of 3.45(2)–4.24(2) Å. In the second position, only one Li–C interaction (2.16(2) Å) is detected; other Li–$C_{toluene}$ distances are 2.84(2)–4.64(2) Å. Thus, despite the structural similarity of **6** with another superbulky lithium carbazolide [*t*-$Bu_2CarbAr_2Li(\eta^6$-Toluene)] (Ar = 3,5-*t*-BuC_6H_3),[19g] where toluene is η^6-coordinated to lithium, in **6**, arene demonstrates a mixed η^1/η^2-coordination mode.

Apparently, a complete symmetrical η^6-coordination in **6** becomes impossible due to the limited volume of the cavity between the aryl substituents.

To estimate numerically the steric saturation of the lithium coordination sphere, the ligand solid angle method[32] has been used, in which the value of the ligand solid angle is equal to the shadowed area percentage of the sphere around the metallocentre. Indeed, while in complex *t*-$Bu_2CarbAr_2Li$(Toluene) (Ar = 3,5-*t*-BuC_6H_3),[19g] the carbazolyl ligand shields the Li cation by only 57.8%, in **6**, the ligand occupies 71.9% of the metal atom coordination sphere. This difference is caused both by the bulkiness and mutual arrangement of the substituents in the aryl fragments, and the position of the metal center relative to the ligand.[32]

Complex **4** containing coordinated *t*-BuLi decomposes completely in a C_6D_{12} solution at 100 °C in 24 h to form a mixture of isobutylene and isobutane in a 70 : 30% (see the SI, Fig. S38). Another major thermolysis product is lithium carbazolide, likely coordinated by cyclohexane-d_{12}.[20] This is likely the result of two parallel reactions: β-hydride abstraction and CH activation. Since cyclohexane is a very weak CH acid, the released isobutylene is a likely substrate for CH activation. Unfortunately, it is not possible to identify other metal-containing products.

DFT results

For complexes **2–4**, QTAIM[33] and NCI[34] analyses were performed at the DLPNO-CCSD(T)/Def2-TZVP//r2-SCAN-3c/Def2-ZVP hybrid theory level (see Computational details in the SI). The resulting molecular graphs with superimposed RDG function isosurfaces are presented in Fig. 5 and S40 in the SI. The QTAIM molecular graph demonstrates two bonding pathways between the anionic carbon atom and both lithium atoms. According to the ratio of QTAIM parameters $\rho(r)$, $\Delta\rho(r)$, and $H(r)$, the Li2–C(R) and Li1–C(R) bonds are of the same dative nature. In Bader's terminology,[33] these interactions are intermediate, and it is important that the $H(r)$ value is small but positive. The strength of the Li–C bonds differs and correlates with the bond length (Table 2), with Li2–C(R) being ~3 kcal mol^{-1} stronger than Li1–C(R) in cases **2** and **3**, but weaker by ~2 times in **4**. This difference is due to varying degrees of coordination unsaturation, which is lower for Li1 due to strong

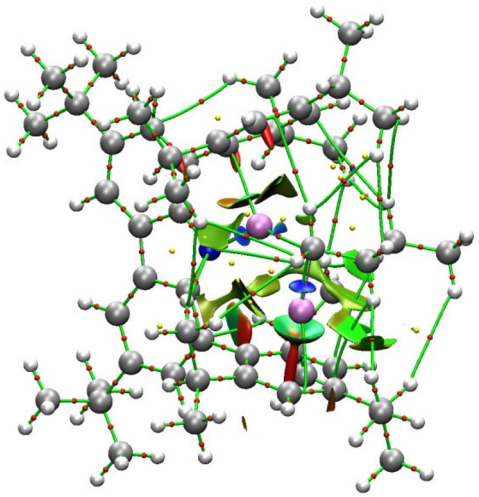

Fig. 5 The fragment for the RDG isosurface (isovalue is 0.5 a.u) combined with the QTAIM molecular graph for compound **2** at the DLPNO-CCSD(T)/Def2-TZVP level.

(13.2–13.5 kcal mol^{-1}) Li1···N coordination. In complexes **2** and **3**, the Li1 atom is bonded to the C_{ipso} atom of the Tipp-substituent, with an interaction strength of 2.3–3.0 kcal mol^{-1}, similar to previously studied complexes.[20] In compound **4**, a Li···C_{ipso} contact is also present (visible in the RDG function in Fig. S40), but it is too weak to localize a BCP (3; −1). The Li2 atom interacts with the phenyl ring of the Tipp-substituent. Notably, based on the shortest interatomic distances, only one bonding pathway Li2···C(arene) was localized for **2** and **3**, and two for **4**. Its strength amounts to 4.8–5.3 kcal mol^{-1}, which is significantly higher than that of Li1···C_{ipso}. However, the displacement of the Li2 atom relative to the normal from the center of the arene cycle is very small (0.037, 0.042, and 0.023 Å for optimized **2**, **3**, and **4**, respectively). This indicates η^6-coordination of Li···arene, which is confirmed by the RDG function isosurface, having a plate-like appearance uniform in all six Li2···C(arene) directions (Fig. 5).

The second factor of the difference in interactions with Li atoms across series **2**, **3**, and **4** is the increase in the cavity between the Tipp substituents, which can be easily numerically estimated through the distances between two C_{ipso}(Tipp) atoms, equal to 5.823, 5.826, and 6.009 Å in optimized molecules **2**, **3**, and **4**, respectively. It is worth noting that the total strength of a complex mesh of H···H and C···H contacts between R- and Tipp-substituents for **2–4** varies within a narrow range (8.5–9.6 kcal mol^{-1}), despite the substituents being very different in terms of the spatial structure and steric hindrance. It seems that cavity expansion is also affecting this.

The results of QTAIM and NCI analyses for complex **5** were reported by us previously.[20] As expected, complex **6** exhibits topological parameters very similar to **5** (Table 2). Among these, it should be noted that the strength of the Li···arene coordination is 3.6 and 3.7 kcal mol^{-1} in **5** and **6**, respectively, while the Li···N and Li···C_{ipso} interactions are slightly shorter and stronger than in **2–4**. This indicates that the coordination

Table 2 QTAIM data for Li···C and Li···N interactions in optimized molecules **2–6** at the DLPNO-CCSD(T)/Def2-TZVP//r^2-SCAN-3c/Def2-TZVP level

Compound	Connected atoms	Distance	ρ, a.u.	$\Delta\rho$, a.u.	$V(r)$, a.u.	$H(r)$, a.u.	E_{cont}, kcal mol^{-1}
2	Li1···N	1.955	0.03418	0.22923	−0.04236	0.00747	13.3
	Li1···C$_{ipso}$	2.442	0.01089	0.05998	−0.00945	0.00277	3.0
	Li1–C(*n*-Bu)	2.115	0.02938	0.14833	−0.03066	0.00321	9.6
	Li2–C(*n*-Bu)	2.029	0.03514	0.18266	−0.03916	0.00325	12.3
	Li2···C(arene)	2.336	0.01594	0.09751	−0.01705	0.00366	5.3
	∑(C···H + C···C)[a]						8.5
3	Li1···N	1.952	0.03473	0.23205	0.00747	−0.04308	13.5
	Li1···C$_{ipso}$	2.528	0.00893	0.04875	0.00240	−0.00739	2.3
	Li1–C(CH$_2$SiMe$_3$)	2.141	0.02680	0.13596	0.00338	−0.02724	8.5
	Li2–C(CH$_2$SiMe$_3$)	2.046	0.03180	0.17009	0.00376	−0.03500	11.0
	Li2···C(arene)	2.375	0.01477	0.08865	0.00346	−0.01524	4.8
	∑(C···H, C···C)[a]						9.6
4	Li1···N	1.963	0.03419	0.22585	0.00727	−0.04192	13.2
	Li1···C$_{ipso}$	2.811	—	—	—	—	—
	Li1–C(*t*-Bu)	2.184	0.02524	0.12471	0.00297	−0.02523	7.9
	Li2–C(*t*-Bu)	2.331	0.01609	0.09906	0.00377	−0.01722	5.4
	Li2···C(arene)	2.339	0.01587	0.09823	0.00377	−0.01702	5.3
	Li2···C(arene)	2.331	0.01609	0.09906	0.00377	−0.01722	5.4
	∑(C···H, C···C)[a]						9.1
5 [20]	Li···N	1.914	0.03832	0.25957	−0.04925	0.00782	15.5
	Li···C$_{ipso}$	2.381	0.01283	0.07105	−0.01156	0.00310	3.6
	Li···C(benzene)	2.324	0.01283	0.07221	−0.01146	0.00330	3.6
	∑(C···H + C···C)[b]						7.4
6	Li···N	1.915	0.03830	0.25921	0.00781	−0.04919	15.4
	Li···C$_{ipso}$	2.377	0.01303	0.07317	0.00320	−0.01189	3.7
	Li···C(toluene)	2.384	0.01286	0.07145	0.00324	−0.01137	3.6
	∑(C···H, C···C)[b]						10.9

[a] ∑(C···H, C···C) – sum of C···H and C···C contact strength between R- and Tipp-substituents. [b] ∑(C···H, C···C) – sum of C···H and C···C contact strength between the guest molecule and Tipp-substituents.

unsaturation of the Li atom in **5** and **6** is higher compared to the Li1 atoms in **2–4**.

To explain the nonselectivity of the metalation reaction of **1** with RLi, thermodynamic parameters of elementary steps (reactions (1)–(4) in Table 3) were calculated. According to common chemical views, the N–H group in the presence of R–Li should be fully deprotonated, which is confirmed by negative values of ΔH°_{298} and ΔG°_{298} for reaction (1), varying within the range of −18.4 to −34.2 and −29.0 to −42.7 kcal mol^{-1}, respectively. It should be noted that the deprotonation of **1** under the action of complexes **2–4** (reaction (4)) is thermodynamically highly favorable, and the corresponding ΔH°_{298} and ΔG°_{298} values are of the same order as for reaction (1). Direct formation of **2–4** by reaction (3), apparently proceeds without an intermediate step (2), since the required second fragment R–Li is located near the reaction center due to the fact that RLi exists as an associated species. The Tipp-substituents shield the reaction centers N–H in **1** and Li2–R in **2–4**; therefore, for complexes **2–4** to undergo exchange reaction (4), they must at first dissociate into **1** and RLi, which requires the energy of reaction (2) with the opposite sign. Thermodynamics of reactions (1)–(4) predicts the complete consumption of **1**. All steps (1)–(4) are essentially acid–base interactions, and calculating their activation barriers is impractical. Nevertheless, the effective barrier for reaction (1) is determined by the dissociation energy of the $(RLi)_n$ associate to a monomeric RLi, whereas for reaction (3), it is governed by the dissociation to the dimer $(RLi)_2$. The dissociation energies (ΔG°_{298}) of $(RLi)_n$ to dimers are approximately 5 kcal mol^{-1} lower (Table S4 in the SI); therefore, direct formation of **2–4** (3) seems to be faster compared to (1).

Table 3 Energy values (kcal mol^{-1}) for reactions calculated at the DLPNO-CCSD(T)/Def2-TZVP//r^2-SCAN-3c/Def2-TZVP CPCM(hexane) level

#	R	ΔE_{tot}	ΔH°_{298}	ΔG°_{298}
1 + 1/*n*(RLi)$_n$ = CarbN-Li + RH				
(1)	*n*-Bu	−28.5	−28.4	−37.7
	t-Bu	−33.8	−34.2	−42.7
	CH$_2$SiMe$_3$	−19.0	−18.4	−29.0
CarbN-Li + 1/*n*(RLi)$_n$ = **2**, **3**, or **4**				
(2)	*n*-Bu (**2**)	−7.9	−7.6	−5.3
	t-Bu (**4**)	−5.8	−5.6	−2.4
	CH$_2$SiMe$_3$ (**3**)	−5.6	−5.6	−3.3
CarbNH + 2/*n*(RLi)$_n$ = **2**, **3**, or **4**				
(3)	*n*-Bu (**2**)	−36.4	−36.1	−43.0
	t-Bu (**4**)	−39.6	−39.9	−45.1
	CH$_2$SiMe$_3$ (**3**)	−24.6	−24.0	−32.3
CarbNH + **2**, **3**, or **4** = 2 CarbLi + RH				
(4)	*n*-Bu	−20.6	−20.8	−32.4
	t-Bu	−28.0	−28.6	−40.3
	CH$_2$SiMe$_3$	−13.4	−12.8	−25.6

n = 6 for *n*-Bu and CH$_2$SiMe$_3$, *n* = 4 for *t*-Bu.

It should be noted that QTAIM data show that both Li(1)–C and Li(2)–C are weaker in compound **4** compared to **2** and **3**. This fact rationalizes that **4** is more prone to dissociation (the energy values for the reversed reaction (2) is less for R = *t*-Bu

($\Delta G^{\circ}_{298} = 2.4$ kcal mol^{-1})). Therefore, an additional excess of *t*-BuLi (3 eq.) is required to shift the equilibrium toward **4** in Scheme 2.

In general, DFT results show that the interaction of **1** with RLi obeys thermodynamic control; in particular, the formation of **2–4** is faster than the deprotonation of **1**, which rationalizes the present **2–4** as an admixture and formal incompleteness of the equimolar reaction.

Conclusions

Thus, it was shown that the metalation of superbulky 3,6-di-*tert*-butyl-1,8-bis-(2,4,6-triisopropylphenyl)-9*H*-carbazole with classical organolithium reagents (*n*-BuLi, Me_3SiCH_2Li and *t*-BuLi) does not proceed selectively but affords homobimetallic species as by-products. When the second molar equivalent of alkyl lithium is added, the presence of highly electrophilic and coordinatively unsaturated lithium carbazolide [Carb$^{2,4,6\text{-iPr}}$Li] provokes its total decomposition and the formation of binuclear lithium compounds [Carb$^{2,4,6\text{-iPr}}$Li(μ^2-*n*-BuLi)Li] (**2**), [Carb$^{2,4,6\text{-iPr}}$Li(μ^2-Me_3SiCH_2Li)Li] (**3**), and [Carb$^{2,4,6\text{-iPr}}$Li(*t*-BuLi)Li] (**4**) containing a coordinated monomeric alkyl lithium unit. In contrast, the reaction with solid $[MeLi]_4$ cleanly affords low-coordinate lithium carbazolide and no formation of binuclear complexes was detected even in the presence of excess $[MeLi]_4$. In new complexes, the alkyl carbanion is μ^2-bridging two electrophilic lithium centers in different coordination environments. One lithium is σ-bonded to the carbazolyl ligand *via* the nitrogen atom, while the coordination unsaturation of the second lithium ion is compensated by a series of non-covalent interactions with one flanking the tris(isopropyl)phenyl moiety. Complex **2** is the first structurally characterized compound containing a monomeric *n*-butyl lithium unit. According to QTAIM analysis, in complexes **2–4**, the carbanion fragment has a dative nature for both lithium centers with an energy ranging from 5.4–12.3 kcal mol^{-1}. The weakest binding of the *t*-Bu fragment between two lithium faces is observed in complex **4** (5.4 and 7.9 kcal mol^{-1}), which causes its partial dissociation in a solution of C_6D_6 and cyclohexane-d_{12}. In contrast, complexes **2** and **3** retain their bimetallic structure in C_6D_6 solution. The complexes are inert to CH activation processes, but prolonged heating (C_6H_6, toluene) leads to the decomposition of alkyl lithium fragments, while the released lithium carbazolide traps aromatic substrates.

Experimental

Materials and methods

All operations were carried out in a vacuum or under an atmosphere of argon, using Schlenk techniques or in an argon filled glovebox. After drying over KOH, THF, toluene and benzene were purified by distillation from sodium/benzophenone ketyl. Hexane, heptane, C_6D_6 and C_6D_{12} were dried over the Na/K alloy, transferred under vacuum, and stored over 4 Å molecular sieves in an argon-filled glovebox. *t*-BuLi and *n*-BuLi (2.5 M solution in hexane) were purchased from Aldrich and DalChem company (Russia). 1-Octene, cyclohexene and 1,5-hexadiene were purchased from Aldrich, dried over CaH_2, vacuum-transferred, degassed by two freeze–pump–thaw cycles and kept in a glovebox. 1,8-Dibromo-3,6-di-*tert*-butylcarbazole,[19e] 1-bromo-2,4,6-triisopropylbenzene[35] and Me_3SiCH_2Li[29] were prepared according to literature procedures. Bis[2′-(amino-κ*N*)[1,1′-biphenyl]-2-yl-κ*C*]di-μ-chlorodipalladium (or $PdCl_2$) and Ru-Phos were purchased from DalChem company (Russia).

Spectroscopic methods

^{1}H and ^{13}C NMR spectra were recorded on Bruker Avance 400 (400 and 100 MHz) and Bruker DPX 300 (300 and 75 MHz) instruments, and are internally referenced to residual solvent signals, $CDCl_3$ referenced at δ 7.26 and 77.0 ppm, and C_6D_6 referenced at δ 7.16 and 128.06 ppm. Where required, COSY and HSQC spectra were used to assign NMR spectra. Data for ^{1}H NMR are reported as follows: chemical shift (δ ppm), integration, multiplicity (s = singlet, d = doublet, t = triplet, q = quartet, p = pentet, sext = sextet, hept = heptet, m = multiplet, br s = broad singlet, compl m = complex multiplet), coupling constant (Hz) and assignment. Data for ^{13}C NMR are reported in terms of chemical shift, multiplicity (s = singlet, d = doublet, t = triplet, q = quartet, p = pentet, sext = sextet, hept = heptet, m = multiplet, br. s = broad singlet), and coupling constant (Hz) and no special nomenclature is used for equivalent carbons. IR spectra were recorded as Nujol mulls or KBr pellets on FSM 1201 and Bruker Vertex 70 instruments. A Polaris Q GC/MS spectrometer was used for GS/MS analysis. The N, C, and H elemental analyses were carried out in the microanalytical laboratory of the IOMC using a Carlo Erba Model 1106 elemental analyzer with an accepted tolerance of 0.4 unit on carbon (C), hydrogen (H), and nitrogen (N).

X-ray crystallography

The SC XRD data for **2–4** and **6** were collected with a Rigaku OD Xcalibur E diffractometer (MoKα-radiation, ω-scans technique, λ = 0.71073 Å) using the CrysAlis^{Pro} software package.[36] Numeric (**2–4**) and analytical (**6**) absorption correction was performed using a multifaceted crystal model.[37] The structures were solved *via* an intrinsic phasing algorithm and were refined by full-matrix least squares on F^2 for all data using SHELX.[38,39] All non-hydrogen atoms were found from Fourier syntheses of electron density and refined anisotropically. All hydrogen atoms were placed in calculated positions and refined isotropically with $U(H)_{iso} = 1.2U_{eq}$ ($U(H)_{iso} = 1.5U_{eq}$ for methyl groups). Crystal data and structure refinement parameters are given in Table S1. CCDC 2464354 (**2**), 2464355 (**3**), 2464356 (**4**), and 2464357 (**6**) contain the supplementary crystallographic data for this paper. The corresponding CIFs are also available in the SI.

Calculation details

The geometry optimization for compounds **2–4** was performed at the r^2-SCAN-3c/Def2-TZVP//CPCM(hexane)[8–10] level.[40–42]

Optimized Cartesian coordinates are supplemented as the standard XYZ-file. All calculations were performed using the ORCA v. 6 program.[43] To accelerate the process, the RIJCOSX[44–46] approximation was utilized with the Def2/J[47] fitting basis set. The electron density in WFN format was generated at the DLPNO-CCSD(T)/Def2-TZVP level with TightPNOs.[48–52] QTAIM[33] and NCI[34] analyses were performed using the MultiWFN[53] program. The interaction energy values of contacts were estimated using the Esponosa–Lecomte correlation,[54] where $E_{cont} = -\frac{1}{2}V(r)$. As expected, E_{cont} values (Table 1) are exponentially correlated with inter-atomic distances (Fig. S38). The full molecular graphs for all molecules are the same for the r^2-SCAN-3c and DLPNO-CCSD(T) levels. As components of NCI analysis, the RDG function and the sign of eigenvalue λ_2 (Fig. S39) were visualized using the VMD program[55] with standard parameters[56] (isovalue 0.05 a.u., λ_2 coloring in the blue-green-red pallet ranges from −0.035 to 0.02 a.u.).

Synthesis of 3,6-di-*tert*-butyl-1,8-bis-(2,4,6-triisopropylphenyl)-9*H*-carbazole (1). A solution of Grignard reagent in THF (50 ml), obtained from 1-bromo-2,4,6-triisopropylbenzene (10.36 g, 36.65 mmol) and magnesium (1.05 g, 44.93 mmol), was added to a solution of $ZnCl_2$ (5.00 g, 36.65 mmol) in THF (20 ml) and stirred for an additional 2 h. The resulting organozinc reagent was then added to a solid mixture of 1,8-dibromo-3,6-di-*tert*-butylcarbazole (4.00 g, 9.15 mmol), palladium catalyst (0.06 g, 0.09 mmol, 1 mol%) and Ru-Phos (0.09 g, 0.09 mmol, 1 mol%) at room temperature. The reaction mixture was heated at 70 °C for 48 h. Afterwards, the brownish mixture was allowed to cool to ambient temperature and transferred to a separation funnel. Then 100 ml of deionized water and 100 ml of ether were added. Phases were separated, the aqueous phase was extracted with 2 × 50 ml of diethyl ether and the combined organic phases were washed once with 50 ml of water. The organic phase was dried over $MgSO_4$ and the volatiles were removed on a rotary evaporator, to afford a brown oil. The oil was evacuated at 100 °C, and excess triisopropylbenzene was separated in the receiver. The brown semi-solid was redissolved in hexane and purified by flash chromatography on silica gel (eluent 100% hexane). The resulting solid was recrystallized from heptane, giving the target carbazole **1** in 80% yield as colorless crystals (5.00 g). **^{1}H NMR (400 MHz, $CDCl_3$, 298 K):** δ 8.13 (d, 2H, 4,5-CH-carbazolyl, $^4J_{HH}$ = 1.9 Hz), 7.39 (br s, 1H, NH), 7.15 (d, 2H, 2,7-CH-carbazolyl, $^4J_{HH}$ = 1.9 Hz), 7.08 (s, 4H, CH-Ar), 2.97 (hept, 2H, *p*-C*H*$(CH_3)_2$, $^3J_{HH}$ = 7.2 Hz), 2.46 (hept, 4H, *o*-C*H*$(CH_3)_2$, $^3J_{HH}$ = 6.9 Hz), 1.44 (s, 18H, *t*Bu), 1.33 (d, 12H, *p*-CH(C$H_3)_2$, $^3J_{HH}$ = 7.0 Hz), 0.99 (d, 12H, *o*-CH(C$H_3)_2$, $^3J_{HH}$ = 6.9 Hz), 0.94 (d, 12H, *o*-CH(C$H_3)_2$, $^3J_{HH}$ = 6.9 Hz). **^{13}C{^{1}H} NMR (100 MHz, $CDCl_3$, 298 K):** δ 148.34 (s, *ipso*-C-aryl), 147.78 (s, *ipso*-C-aryl), 142.26 (s, C-carbazolyl), 136.89 (s, C-carbazolyl), 133.38 (s, *ipso*-C-aryl), 126.48 (s, CH-carbazolyl), 122.91 (s, C-carbazolyl), 122.59 (s, C-carbazolyl), 120.95 (s, 3,5-CH-aryl), 114.32 (s, CH-carbazolyl), 34.63 (s, *C*$(CH_3)_3$-carbazolyl), 34.16 (s, *p*-*C*H$(CH_3)_2$), 31.93 (s, C(*C*$H_3)_3$-carbazolyl), 30.53 (s, *o*-*C*H$(CH_3)_2$), 24.72 (s, *o*-CH(*C*$H_3)_2$), 23.94 (s, *p*-CH(*C*$H_3)_2$), 23.75 (s, *o*-CH(*C*$H_3)_2$). **IR (KBr):** 1588 (s), 1335 (s), 1287 (m), 1265 (m), 1248 (s), 1225 (m), 1188 (s), 1125 (w), 1067 (w), 1022 (s), 957 (m), 866 (s), 837 (s), 810 (s), 694 (m), 642 (m). **Anal. calcd for $C_{50}H_{69}N$ (684.11 g mol^{-1})** C, 87.79; H, 10.17; N 2.05. Found C, 87.82; H, 10.14; N 2.04.

Synthesis of complex [Carb$^{2,4,6\text{-iPr}}$Li(μ^2-*n*-BuLi)Li] (2). *n*-BuLi (1.0 ml of 2.5 M solution in hexane, 2.50 mmol) was added to a solution of 3,6-di-*tert*-butyl-1,8-bis-(2,4,6-triisopropylphenyl)-9*H*-carbazole (0.50 g, 0.73 mmol) in heptane (5 ml) under vacuum at room temperature. The reaction vessel was sealed and the mixture was stirred at RT for 5 days. The resulting light yellow luminescent solution was transferred to a vial. Light yellow-green crystals of complex **2** were obtained by slow concentration of the mother liquor of **2** in heptane. The yield of **2** is 0.44 g (80%). **^{1}H NMR (400 MHz, C_6D_6, 298 K):** δ 8.57 (d, 2H, 4,5-CH-carbazolyl, $^4J_{HH}$ = 2.0 Hz), 7.26 (s, 4H, 3,5-CH-aryl), 7.14 (d, 2H, 2,7-CH-carbazolyl, $^4J_{HH}$ = 2.0 Hz), 3.02 (hept, 4H, *o*-C*H*$(CH_3)_2$, $^3J_{HH}$ = 6.7 Hz), 2.84–2.73 (m, 2H, *p*-C*H*$(CH_3)_2$), 1.55 (s, 18H, *t*Bu-carbazolyl), 1.25–1.19 (compl m, 14H, *p*-CH(C$H_3)_2$ and CH_2-*n*-BuLi), 1.15–1.05 (compl m, 14H, *o*-CH(C$H_3)_2$ and CH_2-*n*-BuLi), 1.03–0.95 (compl m, 15H, *o*-CH(C$H_3)_2$ and CH_3-*n*-BuLi), −1.71 (t, 2H, $LiCH_2$, $^3J_{HH}$ = 8.4 Hz). **^{13}C{^{1}H} NMR (100 MHz, C_6D_6, 298 K):** δ 149.95 (s, *ipso*-C-aryl), 149.58 (s, *ipso*-C-aryl), 149.52 (s, C-carbazolyl), 138.79 (s, C-carbazolyl), 136.98 (s, *ipso*-C-aryl), 125.26 (s, C-carbazolyl), 122.92 (s, C-carbazolyl), 122.03 (s, 3,5-CH-aryl), 122.00 (s, CH-carbazolyl), 115.26 (s, CH-carbazolyl), 34.33 (s, *C*$(CH_3)_3$-carbazolyl), 34.10 (s, *p*-*C*H$(CH_3)_2$), 33.50 (s, CH_2), 32.20 (s, C(*C*$H_3)_3$-carbazolyl), 31.90 (s, CH_2), 30.43 (s, *o*-*C*H$(CH_3)_2$), 24.46 (s, *o*-CH(*C*$H_3)_2$), 23.80 (s, *o*-CH(*C*$H_3)_2$), 23.49 (*p*-CH(*C*$H_3)_2$), 14.09 (s, CH_3), 7.48 (br s, $LiCH_2$). **^{7}Li NMR (100 MHz, C_6D_6, 298 K):** δ −1.04. **IR (KBr):** 1747 (m), 1603 (m), 1305 (s), 1267 (s), 1235 (s) 1186 (s), 1107 (s), 1057 (s), 1036 (s), 939 (s), 864 (s), 845 (m), 773 (s), 723 (s), 673 (s). **Anal. calcd for $C_{54}H_{77}Li_2N$ (754.10 g mol^{-1})** C, 86.01; H, 10.29; N 1.86. Found C, 86.50; H, 10.43; N 1.80.

Synthesis of complex [Carb$^{2,4,6\text{-iPr}}$Li(μ^2-Me$_3$SiCH$_2$Li)Li] (3). Me_3SiCH_2Li (0.24 g, 2.50 mmol) was added to a solution of 3,6-di-*tert*-butyl-1,8-bis-(2,4,6-triisopropylphenyl)-9*H*-carbazole (0.50 g, 0.73 mmol) in heptane (5 ml) under vacuum at room temperature. The reaction vessel was sealed and the mixture was stirred at RT for 5 days. The resulting light yellow luminescent solution was transferred into a vial. Light yellow-green crystals of complex **3** were obtained by slow concentration of the mother liquor of **3** in heptane. The yield of **3** is 0.52 g (90%). **^{1}H NMR (400 MHz, C_6D_6, 298 K):** δ 8.53 (d, 2H, 4,5-CH-carbazolyl, $^4J_{HH}$ = 1.8 Hz), 7.24 (s, 4H, 3,5-CH-aryl), 7.06 (d, 2H, 2,7-CH-carbazolyl, $^4J_{HH}$ = 1.8 Hz), 3.08–2.95 (m, 4H, *o*-C*H*$(CH_3)_2$), 2.93–2.81 (m, 2H, *p*-C*H*$(CH_3)_2$), 1.49 (s, 18H, *t*Bu-carbazolyl), 1.19 (d, 12H, *p*-CH(C$H_3)_2$, $^3J_{HH}$ = 6.9 Hz), 1.10 (d, 12H, *o*-CH(C$H_3)_2$, $^3J_{HH}$ = 6.8 Hz), 0.98 (d, 12H, *o*-CH(C$H_3)_2$, $^3J_{HH}$ = 6.9 Hz), 0.00 (s, 9H, $SiMe_3$), −2.97 (s, 2H, $LiCH_2$). **^{13}C{^{1}H} NMR (100 MHz, C_6D_6, 298 K):** δ 149.77 (s, *ipso*-C-aryl), 149.68 (s, *ipso*-C-aryl), 149.14 (s, C-carbazolyl), 139.37 (s, C-carbazolyl), 137.02 (s, *ipso*-C-aryl), 126.24 (s, C-carbazolyl), 123.11 (s, CH-carbazolyl), 122.05 (s, C-carbazolyl), 121.96 (s, 3,5-CH-aryl), 115.29 (s, CH-carbazolyl), 34.31 (s, *C*$(CH_3)_3$-carbazolyl), 33.67 (s, *p*-*C*H$(CH_3)_2$), 32.17 (s, C(*C*$H_3)_3$-carbazolyl),

30.45 (s, *o*-C*H*(CH$_3$)$_2$), 24.44 (s, *o*-CH(C*H*$_3$)$_2$), 24.07 (s, *o*-CH(C*H*$_3$)$_2$), 23.36 (*p*-CH(C*H*$_3$)$_2$), 4.30 (s, SiMe$_3$), −9.17 (br s, LiCH$_2$). **^{7}Li NMR (100 MHz, C$_6$D$_6$, 298 K):** δ −1.34. **^{29}Si NMR (79.5 MHz, C$_6$D$_6$, 298 K):** δ −1.81. **IR (KBr):** 1742 (s), 1603 (s), 1592 (s), 1545 (s), 1457 (s), 1308 (s), 1269 (s), 1238 (s), 1202 (s), 1169 (s), 1109 (s), 1057 (s), 1036 (s), 976 (m), 939 (s), 864 (s), 818 (s), 775 (s), 725 (s), 673 (s). **Anal. calcd for C$_{52}$H$_{79}$Li$_2$NSi (784.20 g mol^{-1})** C, 82.71; H, 10.15; N 1.79. Found C, 82.90; H, 10.20; N 1.68.

Synthesis of complex [Carb$^{2,4,6\text{-iPr}}$Li(μ^2-*t*-BuLi)] (4). *t*-BuLi (1.8 ml of 1.7 M solution in hexane, 3.00 mmol) was added to a solution of 3,6-di-*tert*-butyl-1,8-bis-(2,4,6-triisopropylphenyl)-9*H*-carbazole (0.50 g, 0.73 mmol) in heptane (5 ml) under vacuum at room temperature. The reaction vessel was sealed and the mixture was stirred at RT for 5 days. The resulting light yellow luminescent solution was transferred into a vial. Light yellow-green crystals of complex **4** were obtained by slow concentration of the mother liquor of **4** in heptane. The yield of **4** is 0.32 g (58%). **^{1}H NMR (400 MHz, C$_6$D$_{12}$, 298 K):** δ 8.14 (d, 2H, 4,5-CH-carbazolyl, $^4J_{HH}$ = 2.0 Hz), 7.23 (s, 4H, 3,5-CH-aryl), 6.71 (d, 2H, 2,7-CH-carbazolyl, $^4J_{HH}$ = 2.0 Hz), 3.04–2.80 (m, 4H, *o*-C*H*(CH$_3$)$_2$), 2.80–2.62 (m, 2H, *p*-C*H*(CH$_3$)$_2$), 1.45 (s, 18H, *t*Bu-carbazolyl), 1.34 (d, 12H, *o*-CH(C*H*$_3$)$_2$, $^3J_{HH}$ = 7.0 Hz), 1.11–0.97 (compl m, 24H, *o*-CH(C*H*$_3$)$_2$ and *p*-CH(C*H*$_3$)$_2$), 0.24 (s, 9H, LiC(C*H*$_3$)$_3$). **^{13}C{^{1}H} NMR (100 MHz, C$_6$D$_{12}$, 298 K):** δ 149.72 (s, *ipso*-C-aryl), 149.29 (s, *ipso*-C-aryl), 148.47 (s, C-carbazolyl), 139.94 (s, C-carbazolyl), 135.78 (s, *ipso*-C-aryl), 126.34 (s, C-carbazolyl), 123.39 (s, C-carbazolyl), 121.73 (s, 3,5-CH-aryl), 121.19 (s, CH-carbazolyl), 114.83 (s, CH-carbazolyl), 34.16 (s, *C*(CH$_3$)$_3$-carbazolyl), 33.83 (s, *p*-*C*H(CH$_3$)$_2$), 33.47 (s, Li–C(*C*H$_3$)$_3$), 31.76 (s, C(*C*H$_3$)$_3$-carbazolyl), 30.31 (s, *o*-*C*H(CH$_3$)$_2$), 23.91 (s, *o*-CH(*C*H$_3$)$_2$), 23.60 (s, *o*-CH(*C*H$_3$)$_2$), 23.16 (*p*-CH(*C*H$_3$)$_2$), 13.30 (br s, Li*C*(CH$_3$)$_3$). **^{7}Li NMR (100 MHz, C$_6$D$_{12}$, 298 K):** δ −1.47. **IR (KBr):** 1760 (m), 1592 (s), 1543 (m), 1408 (s), 1306 (s), 1264 (s), 1233 (s), 1206 (m), 1175 (s), 1126 (s), 1103 (m), 1055 (s), 1036 (s), 960 (m), 943 (m), 893 (m), 866 (s), 843 (m), 773 (s). **Anal. calcd for C$_{54}$H$_{77}$Li$_2$N (754.10 g mol^{-1})** C, 86.01; H, 10.29; N 1.86. Found C, 86.45; H, 10.43; N 1.70.

Synthesis of [Carb$^{2,4,6\text{-iPr}3}$]Li(C$_6$H$_6$) (5). Method 1. Complex **4** (0.50 g, 0.66 mmol) was dissolved in 10 ml of benzene and slowly concentrated to 1 ml. Pale yellow-green crystals of **5** were separated from the mother liquor. The yield of **5** is 0.12 g (22%). **Method 2.** Complex **2** (0.50 g, 0.66 mmol) was dissolved in 10 ml of benzene and heated at 100 °C for 48 h. Light yellow-green crystals of **5** were obtained by slow concentration of the mother liquor in benzene at RT. The yield of **5** is 0.31 g (56%). **^{1}H NMR (400 MHz, C$_6$D$_6$, 298 K):** δ 8.51 (d, 2H, 4,5-CH-carbazolyl, $^4J_{HH}$ = 1.8 Hz), 7.27 (d, 2H, 2,7-CH-carbazolyl), 7.13 (s, 12H, CH-benzene), 7.04 (s, 4H, 3,5-CH-aryl), 2.97 (hept, 4H, *o*-C*H*(CH$_3$)$_2$, $^3J_{HH}$ = 6.7 Hz), 2.72–2.59 (m, 2H, *p*-C*H*(CH$_3$)$_2$), 1.56 (s, 18H, *t*Bu-carbazolyl), 1.14 (d, 12H, *o*-CH(C*H*$_3$)$_2$, $^3J_{HH}$ = 6.9 Hz), 1.11 (d, 12H, *p*-CH(C*H*$_3$)$_2$, $^3J_{HH}$ = 7.0 Hz), 0.87 (d, 24H, *o*-CH(C*H*$_3$)$_2$, $^3J_{HH}$ = 6.9 Hz). **^{13}C{^{1}H} NMR (100 MHz, C$_6$D$_6$, 298 K):** δ 149.91 (s, *ipso*-C-aryl), 148.48 (s, *ipso*-C-aryl), 148.12 (s, C-carbazolyl), 138.75 (s, C-carbazolyl), 136.96 (s, *ipso*-C-aryl), 128.22 (s, CH-benzene), 125.84 (s, C-carbazolyl), 123.45 (s, C-carbazolyl), 122.59 (s, CH-carbazolyl), 121.10 (s, 3,5-CH-aryl), 115.09 (s, CH-carbazolyl), 34.43 (s, *C*(CH$_3$)$_3$-carbazolyl), 33.96 (s, *p*-*C*H(CH$_3$)$_2$), 32.31 (s, C(*C*H$_3$)$_3$-carbazolyl), 30.27 (s, *o*-*C*H(CH$_3$)$_2$), 25.09 (s, *o*-CH(*C*H$_3$)$_2$), 23.91 (s, *o*-CH(*C*H$_3$)$_2$), 23.75 (*p*-CH(*C*H$_3$)$_2$). **^{7}Li NMR (100 MHz, C$_6$D$_6$, 298 K):** δ −1.31. **IR (KBr):** 1736 (w), 1599 (s), 1557 (s), 1304 (s), 1279 (s), 1235 (s), 1201 (m), 1188 (m), 1169 (m), 1107 (s), 1051 (m), 1034 (m), 941 (m), 862 (s), 791 (s), 777 (s), 721 (s), 669 (s), 657 (s). **Anal. calcd for C$_{62}$H$_{80}$LiN (846.27 g mol^{-1})** C, 88.00; H, 9.53; N 1.66. Found C, 88.23; H, 9.70; N 1.60.

Synthesis of [Carb$^{2,4,6\text{-iPr}3}$]Li(C$_7$H$_8$) (6). Complex **3** (0.50 g, 0.63 mmol) was dissolved in 10 ml of toluene and heated at 100 °C for 48 h. The volatiles were removed under vacuum and the solid residue was redissolved in heptane (10 ml). Light yellow-green crystals of complex **6** were obtained by slow concentration of the mother liquor in benzene at RT. The yield of **6** is 0.37 g (75%). **^{1}H NMR (400 MHz, C$_6$D$_6$, 298 K):** δ 8.51 (d, 2H, 4,5-CH-carbazolyl, $^4J_{HH}$ = 1.8 Hz), 7.27 (d, 2H, 2,7-CH-carbazolyl), 7.12–6.94 (compl m, 9H, CH-toluene and 3,5-CH-aryl), 3.03–2.91 (m, 4H, *o*-C*H*(CH$_3$)$_2$), 2.72–2.60 (m, 2H, *p*-C*H*(CH$_3$)$_2$), 2.09 (s, 3H, CH$_3$-toluene), 1.55 (s, 18H, *t*Bu-carbazolyl), 1.14 (d, 12H, *o*-CH(C*H*$_3$)$_2$, $^3J_{HH}$ = 6.8 Hz), 1.10 (d, 12H, *p*-CH(C*H*$_3$)$_2$, $^3J_{HH}$ = 7.0 Hz), 0.87 (d, 24H, *o*-CH(C*H*$_3$)$_2$, $^3J_{HH}$ = 6.9 Hz). **^{13}C{^{1}H} NMR (100 MHz, C$_6$D$_6$, 298 K):** δ 149.91 (s, *ipso*-C-aryl), 148.49 (s, *ipso*-C-aryl), 148.09 (s, C-carbazolyl), 138.77 (s, C-carbazolyl), 137.52 (s, *ipso*-C-toluene), 136.96 (s, *ipso*-C-aryl), 128.96 (s, CH-toluene), 128.19 (s, CH-toluene), 125.85 (s, C-carbazolyl), 125.32 (s, CH-toluene), 123.45 (s, C-carbazolyl), 122.59 (s, CH-carbazolyl), 121.09 (s, 3,5-CH-aryl), 115.09 (s, CH-carbazolyl), 34.43 (s, *C*(CH$_3$)$_3$-carbazolyl), 33.96 (s, *p*-*C*H(CH$_3$)$_2$), 32.30 (s, C(*C*H$_3$)$_3$-carbazolyl), 30.27 (s, *o*-*C*H(CH$_3$)$_2$), 25.09 (s, *o*-CH(*C*H$_3$)$_2$), 23.90 (s, *o*-CH(*C*H$_3$)$_2$), 23.75 (*p*-CH(*C*H$_3$)$_2$), 21.06 (s, CH$_3$-toluene). **^{7}Li NMR (100 MHz, C$_6$D$_6$, 298 K):** δ −1.31. **IR (KBr):** 1758 (m), 1603 (s), 1561 (m), 1306 (s), 1286 (s), 1269 (s), 1236 (s), 1204 (m), 1169 (m), 1105 (s), 1069 (m), 1034 (s), 957 (m), 939 (s), 870 (s), 847 (s), 787 (m), 773 (s), 696 (s), 656 (s). **Anal. calcd for C$_{57}$H$_{76}$LiN (782.18 g mol^{-1})** C, 87.53; H, 9.79; N 1.79. Found C, 88.11; H, 9.91; N 1.63.

Thermolysis of complex 4. Complex **4** (0.05 g, 0.07 mmol) was placed in an NMR ampule and dissolved in cyclohexane-d$_{12}$ (0.50 ml). The sample was heated at 100 °C for 24 hours. The released isobutylene and isobutane were identified by GC/MS.

Author contributions

A. N. S. and A. A. T. conceived and directed the project. M. A. B. performed the synthetic experiments. A. V. C. performed X-ray analysis. A. N. S. and A. A. T. wrote the manuscript with assistance from all authors.

Conflicts of interest

The authors declare no conflict of interest.

Data availability

The data that support the findings of this study are available in the supplementary information (SI) of this manuscript or by contacting the authors.

Supplementary information: synthetic procedures, spectroscopic data, computational and crystallographic details. See DOI: https://doi.org/10.1039/d5dt02800k.

CCDC 2464354 (**2**), 2464355 (**3**), 2464356 (**4**) and 2464357 (**6**) contain the supplementary crystallographic data for this paper.[57a–d]

Acknowledgements

The financial support from the Russian Science Foundation is highly acknowledged (Project No. 23-73-10148). The SC XRD data were obtained using the equipment of the Center for Collective Use "Analytical Center of the IOMC RAS". DFT calculations were performed using the equipment of the Center for Collective Use of INEOS RAS.

References

1 W. Schlenk and J. Holtz, *Ber. Dtsch. Chem. Ges.*, 1917, **50**, 262–274.
2 (*a*) U. Wietelmann and J. Klett, *Z. Anorg. Allg. Chem.*, 2018, **644**, 194–204; (*b*) F. Totter and P. Rittmeyer, in *Organometallics in Synthesis*, ed. M. Schlosser, Wiley, New York, 1994; (*c*) *The Chemistry of Organolithium compounds*, ed. Z. Rappoport and I. Marek, Wiley, New York, 2004; (*d*) *Lithium Compounds in Organic Synthesis—From Fundamentals to Applications*, ed. R. Luisi and V. Capriati, Wiley-VCH, Weinheim, 2014; (*e*) F. Totter and P. Rittmeyer, Organolithium Compounds – Industrial Applications and Handling, in *Organometallics in Synthesis, A Manual*, ed. M. Schlosser, Wiley, New York, 1994, vol. 2, pp. 167–194; (*f*) J.-M. Tarascon, *Nat. Chem.*, 2010, **2**, 510.
3 G. Wu and M. Huang, *Chem. Rev.*, 2006, **106**, 2596–2616.
4 V. Snieckus, *Chem. Rev.*, 1990, **90**, 879–933.
5 B. Wei, Yi.-H. Chen and P. Knochel, *Acc. Chem. Res.*, 2024, **57**, 1951–1963.
6 (*a*) H. J. Reich, *Chem. Rev.*, 2013, **113**, 7130; (*b*) L. Knauer, J. Wattenberg, U. Kroesen and C. Strohmann, *Dalton Trans.*, 2019, **48**, 11285–11291; (*c*) A. Münch, L. Knauer, H. Ott, C. Sindlinger, R. Herbst-Irmer, C. Strohmann and D. Stalke, *J. Am. Chem. Soc.*, 2020, **142**, 15897–15906; (*d*) N. Davison and E. Lu, *Dalton Trans.*, 2023, **52**, 8172–8192; (*e*) A. Harrison-Marchand and F. Mongin, *Chem. Rev.*, 2013, **113**, 7470–7562; (*f*) R. A. Gossage, J. T. B. H. Jatrzebski and G. van Koten, *Angew. Chem., Int. Ed.*, 2005, **44**, 1448–1454.
7 V. H. Gessner, C. Däschlein and C. Strohmann, *Chem. – Eur. J.*, 2009, **15**, 3320–3334.
8 (*a*) E. Weiss and E. A. C. Lucken, *J. Organomet. Chem.*, 1964, **2**, 197–205; (*b*) E. Weiss and G. Henken, *J. Organomet. Chem.*, 1970, **21**, 265–268.
9 (*a*) T. Kotrke and D. Stalke, *Angew. Chem., Int. Ed. Engl.*, 1993, **32**, 580–582; (*b*) H. Dietrich, *Acta Crystallogr.*, 1963, **16**, 681–689; (*c*) H. J. Dietrich, *J. Organomet. Chem.*, 1981, **205**, 291–299.
10 (*a*) U. Siemeling, T. Redecker, B. Neumann and H.-G. Stammler, *J. Am. Chem. Soc.*, 1994, **116**, 5507–5508; (*b*) R. Zerger, W. Rhine and G. Stucky, *J. Am. Chem. Soc.*, 1974, **96**, 6048–6055; (*c*) A. F. M. Maqsudur Rahman and J. P. Oliver, *J. Organomet. Chem.*, 1986, **317**, 267–275; (*d*) J. O. Bauer, *Z. Kristallogr. - New Cryst. Struct.*, 2020, **235**, 353–356.
11 O. Tai, R. Hopson and P. G. Williard, *Org. Lett.*, 2017, **19**, 3966–3969.
12 N. Davison, C. L. McMullin, L. Zhang, S.-X. Hu, P. G. Waddell, C. Wills, C. Dixon and E. Lu, *J. Am. Chem. Soc.*, 2023, **145**, 6562–6576.
13 (*a*) N. Davison, E. Falbo, P. G. Waddell, T. J. Penfold and E. Lu, *Chem. Commun.*, 2021, **57**, 6205–6208; (*b*) J. Lebon, A. Mortis, C. Maichle-Mössmer, M. Manßen, P. Sirsch and R. Anwander, *Angew. Chem., Int. Ed.*, 2023, **62**, e202214599.
14 (*a*) T. Tatic, H. Ott and D. Stalke, *Eur. J. Inorg. Chem.*, 2008, 3765–3768; (*b*) N. Davison, P. G. Waddell, C. Dixon, C. Wills, T. J. Penfold and E. Lu, *Dalton Trans.*, 2022, **51**, 10707–10713.
15 (*a*) J. Kleinheider, T. Schrimpf, R. Scheel, T. Mairath, A. Hermann, K. Knepper and C. Strohmann, *Chem. – Eur. J.*, 2024, **30**, e202304226; (*b*) C. Strohmann, T. Seibel and K. Strohfeldt, *Angew. Chem., Int. Ed.*, 2003, **42**, 4531–4533; (*c*) C. Strohmann and V. H. Gessner, *Angew. Chem., Int. Ed.*, 2007, **46**, 8281–8283; (*d*) V. H. Gessner and C. Strohmann, *J. Am. Chem. Soc.*, 2008, **130**, 14412–14413; (*e*) M. Hülsmann, A. Mix, B. Neumann, H.-G. Stammler and N. W. Mitzel, *Eur. J. Inorg. Chem.*, 2014, 46–50.
16 (*a*) B. Walfort, L. Lameyer, W. Weiss, R. Herbst-Irmer, R. Bertermann, J. Rocha and D. Stalke, *Chem. – Eur. J.*, 2001, **7**, 1417–1423; (*b*) M. Pérez-Jiménez, J. Campos, J. Jover, S. Álvarez and E. Carmona, *Angew. Chem., Int. Ed.*, 2022, **61**, e202116009; (*c*) K. Ruhlandt-Senge, J. J. Ellison, R. J. Wehmschulte, F. Pauer and P. P. Power, *J. Am. Chem. Soc.*, 1993, **115**, 11353–11357.
17 (*a*) M. A. Nichols and P. C. Williard, *J. Am. Chem. Soc.*, 1993, **115**, 1568–1572; (*b*) C. Strohmann, K. Strohfeldt and D. Schildbach, *J. Am. Chem. Soc.*, 2003, **125**, 13672–13673; (*c*) C. Strohmann and V. H. Gessner, *Angew. Chem., Int. Ed.*, 2007, **46**, 4566–4569.
18 (*a*) D. L. Kays, *Chem. Soc. Rev.*, 2016, **45**, 1004–1018; (*b*) H. B. Mansaray, M. Kelly, D. Vidovic and S. Aldridge, *Chem. – Eur. J.*, 2011, **17**, 5381–5386; (*c*) A. J. Blake, W. Lewis, J. McMaster, R. S. Moorhouse, G. J. Moxey and D. L. Kays, *Dalton Trans.*, 2011, **40**, 1641–1645; (*d*) R. S. Moorhouse, G. J. Moxey, F. Ortu, T. J. Reade, W. Lewis, A. J. Blake and D. L. Kays, *Inorg. Chem.*, 2013, **52**, 2678–2683; (*e*) I. V. Basalov, S. C. Roşca, D. M. Lyubov, A. N. Selikhov, G. K. Fukin, Y. Sarazin, J.-F. Carpentier and A. A. Trifonov, *Inorg. Chem.*, 2014, **53**, 1654–1661; (*f*) A. N. Selikhov, A. V. Cherkasov, G. K. Fukin,

A. A. Trifonov, I. del Rosal and L. Maron, *Organometallics*, 2015, **34**, 555–562; (*g*) A. N. Selikhov, T. V. Mahrova, A. V. Cherkasov, G. K. Fukin, L. Maron and A. A. Trifonov, *Chem. – Eur. J.*, 2017, **23**, 1436–1443; (*h*) A. N. Selikhov, A. V. Cherkasov, A. S. Shavyrin, G. K. Fukin and A. A. Trifonov, *Organometallics*, 2019, **38**, 4615–4624; (*i*) J. Long, A. N. Selikhov, K. A. Lyssenko, Y. Guari, J. Larionova and A. A. Trifonov, *Organometallics*, 2020, **39**, 2785–2790; (*j*) A. N. Selikhov, P. V. Pechenkina, A. V. Cherkasov, Y. V. Nelyubina, T. A. Kovylina and A. A. Trifonov, *Dalton Trans.*, 2022, **51**, 9127–9137; (*k*) J. Long, A. N. Selikhov, N. Yu. Rad'kova, A. V. Cherkasov, Y. Guari, J. Larionova and A. A. Trifonov, *Eur. J. Inorg. Chem.*, 2021, 3008–3012.

19 (*a*) N. D. Coombs, A. Stasch, A. Cowley, A. L. Thompson and S. Aldridge, *Dalton Trans.*, 2008, 332–337; (*b*) A. E. Ashley, A. R. Cowley, J. C. Green, D. R. Johnston, D. J. Watkin and D. L. Kays, *Eur. J. Inorg. Chem.*, 2009, 2547–2552; (*c*) F. Ortu, G. J. Moxey, A. J. Blake, W. Lewis and D. L. Kays, *Chem. – Eur. J.*, 2015, **21**, 6949–6956; (*d*) A. N. Selikhov, M. A. Bogachev, Y. V. Nelyubina, G. Yu. Zhigulin, S. Yu. Ketkov and A. A. Trifonov, *Inorg. Chem. Front.*, 2024, **11**, 4336–4346; (*e*) A. Hinz, *Chem. – Eur. J.*, 2019, **25**, 3267–3271; (*f*) A. Hinz, *Angew. Chem., Int. Ed.*, 2020, **59**, 19065–19069; (*g*) M. Kaiser, M. P. Müller, F. Krätschmer, M. Rutschmann and A. Hinz, *Inorg. Chem. Front.*, 2023, **10**, 2987–2994; (*h*) A. Hinz, L. Winkler and X. Sun, *Chem. Commun.*, 2024, **60**, 11291–11294; (*i*) X. Sun and A. Hinz, *Inorg. Chem.*, 2023, **62**, 10249–10255.

20 M. A. Bogachev, A. N. Selikhov, A. V. Cherkasov, R. R. Aysin, S. S. Bukalov and A. A. Trifonov, *J. Am. Chem. Soc.*, 2025, **147**, 34610–34619.

21 C. Knüpfer, L. Klerner, J. Mai, J. Langer and S. Harder, *Chem. Sci.*, 2024, **15**, 4386–4395.

22 H. Ott, C. Däschlein, D. Leusser, D. Schildbach, T. Seibel, D. Stalke and C. Strohmann, *J. Am. Chem. Soc.*, 2008, **130**, 11901–11911.

23 P. Wijkens, E. M. van Koten, M. D. Janssen, J. T. B. H. Jastrzebski, A. L. Spek and G. van Koten, *Angew. Chem., Int. Ed. Engl.*, 1995, **34**, 219–222.

24 P. Wijkens, J. T. B. H. Jastrzebski, N. Veldman, A. L. Spek and G. van Koten, *Chem. Commun.*, 1997, 2143–2144.

25 J. G. Donkervoort, J. L. Vicario, E. Rijnberg, J. T. B. H. Jastrzebski, H. Kooijman, A. L. Spek and G. van Koten, *J. Organomet. Chem.*, 1998, **550**, 463–467.

26 C. Strohmann and B. C. Abele, *Organometallics*, 2000, **19**, 4173–4175.

27 C. M. P. Kronenburg, E. Rijnberg, J. T. B. H. Jastrzebski, H. Kooijman, M. Lutz, A. L. Spek, R. A. Gossage and G. van Koten, *Chem. – Eur. J.*, 2005, **11**, 253–261.

28 (*a*) N. J. Hardman, B. Twamley, M. Stender, R. Baldwin, S. Hino, B. Schiemenz, S. M. Kauzlarich and P. P. Power, *J. Organomet. Chem.*, 2002, **643–644**, 461–467; (*b*) J. Arnold, V. Knapp, J. A. R. Schmidt and A. Shafir, *J. Chem. Soc., Dalton Trans.*, 2002, 3273–3274.

29 J. W. Connolly and G. Urry, *Inorg. Chem.*, 1963, **2**, 645–646.

30 S. Bywater, P. Lachance and D. J. Worsfold, *J. Phys. Chem.*, 1975, **79**, 2148–2153.

31 B. Schiemen and P. P. Power, *Angew. Chem., Int. Ed. Engl.*, 1996, **35**, 2150–2151.

32 I. A. Guzei and M. Wendt, *Dalton Trans.*, 2006, 3991–3999.

33 R. F. W. Bader, *Atoms in Molecules: A Quantum Theory*, Oxford Univ. Press, Oxford, 1990.

34 E. R. Johnson, S. Keinan, P. Mori-Sánchez, J. Contreras-García, A. Cohen and W. Yang, *J. Am. Chem. Soc.*, 2010, **132**, 6498–6506.

35 G. M. Whitesides, M. Eisenhut and W. M. Bunting, *J. Am. Chem. Soc.*, 1974, **96**, 5398–5407.

36 Rigaku Oxford Diffraction, *CrysAlisPro software system, ver. 43.121a*, Rigaku Corporation, Wroclaw, Poland, 2024.

37 R. C. Clark and J. S. Reid, *Acta Crystallogr., Sect. A: Found. Crystallogr.*, 1995, **51**, 887–897.

38 G. M. Sheldrick, *Acta Crystallogr., Sect. A: Found. Adv.*, 2015, **71**, 3–8.

39 G. M. Sheldrick, *Acta Crystallogr., Sect. C: Struct. Chem.*, 2015, **71**, 3–8.

40 S. Grimme, A. Hansen, S. Ehlert and J.-M. Mewes, *Chem. Phys.*, 2021, **154**, 64–103.

41 C. van. Wüllen, *J. Chem. Phys.*, 1998, **109**, 392–399.

42 F. Weigend and R. Ahlrichs, *Phys. Chem. Chem. Phys.*, 2005, **7**, 3297–3305.

43 F. Neese, F. Wennmohs, U. Becker and C. Riplinger, *J. Chem. Phys.*, 2020, **152**, 224108.

44 F. Neese, *J. Comput. Chem.*, 2003, **24**, 1740–1747.

45 F. Neese, F. Wennmohs, A. Hansen and U. Becker, *Chem. Phys.*, 2009, **356**, 98–109.

46 A. K. Dutta, F. Neese and R. Izsak, *J. Chem. Phys.*, 2016, **144**, 034102.

47 F. Weigend, *Phys. Chem. Chem. Phys.*, 2006, **8**, 1057–1065.

48 C. Riplinger and F. Neese, *J. Chem. Phys.*, 2013, **138**, 034106.

49 C. Riplinger, B. Sandhoefer, A. Hansen and F. Neese, *J. Chem. Phys.*, 2013, **139**, 134101.

50 C. Riplinger, P. Pinski, U. Becker, E. F. Valeev and F. Neese, *J. Chem. Phys.*, 2016, **144**, 024109.

51 M. Saitow, U. Becker, C. Riplinger, E. F. Valeev and F. Neese, *J. Chem. Phys.*, 2017, **146**, 164105.

52 Y. Guo, C. Riplinger, U. Becker, D. G. Liakos, Y. Minenkov, L. Cavallo and F. Neese, *J. Chem. Phys.*, 2018, **148**, 011101.

53 T. Lu, *J. Chem. Phys.*, 2024, **161**, 082503.

54 E. Espinosa, E. Molins and C. Lecomte, *Chem. Phys. Lett.*, 1998, **285**, 170–173.

55 W. Humphrey, A. Dalke and K. Schulten, *J. Mol. Graphics*, 1996, **14**, 33–38.

56 T. Li, *Angew. Chem., Int. Ed.*, 2025, **64**, e202504895.

57 (*a*) CCDC 2464354: Experimental Crystal Structure Determination, 2026, DOI: 10.5517/ccdc.csd.cc2nqc92; (*b*) CCDC 2464355: Experimental Crystal Structure Determination, 2026, DOI: 10.5517/ccdc.csd.cc2nqcb3; (*c*) CCDC 2464356: Experimental Crystal Structure Determination, 2026, DOI: 10.5517/ccdc.csd.cc2nqcc4; (*d*) CCDC 2464357: Experimental Crystal Structure Determination, 2026, DOI: 10.5517/ccdc.csd.cc2nqcd5.